

RHEOLOGY OF DILUTE SUSPENSIONS OF BROWNIAN DIPOLAR AXISYMMETRIC PARTICLES

Y. ALMOG¹ AND I. FRANKEL²

ABSTRACT. We study the respective effects of shear rate and of external field intensity and direction on the contribution to the bulk stress of Brownian dipolar axisymmetric particles suspended in a steady macroscopically homogeneous shear flow of an incompressible Newtonian fluid. Towards this end we obtain the steady orientational distribution and make use of existing general dynamic theories of dilute suspensions. The calculation focuses on the limit of weak rotary diffusion. Thus, unlike previous analyses, the present contribution is not restricted to weak shear effects.

Explicit results are presented for the bulk stress when the external field acts in the plane of the simple shear flow. In cases when the deterministic rotary motion possesses a single sufficiently stable node a simple unified description of the respective effects of both the intensity and azimuthal direction of the external field is provided the boundary-layer approximation. This approximation enables both a qualitative explanation of existing numerical results as well as quantitatively accurate analytical results at relatively moderate values of the rotary Peclet number and the Langevin parameter (~ 10). Furthermore, at still larger values of these parameters use of the present asymptotic approximation is clearly preferable since the numerical schemes rapidly deteriorate when steep orientational gradients appear.

Singularities of the bulk stress are rationalized in terms of the corresponding deterministic rotary motion. This is particularly interesting because some of these singular phenomena (e.g. those associated with an 'intermediate regime' of the field intensity and direction, for which more than one stable attractor exists in the deterministic problem) have no counterparts in suspensions of dipolar spheres or torque-free axisymmetric particles.

Finally, the present results obtained for the orientational distribution are also applicable to the study of other aspects of the macroscale description of suspensions of dipolar axisymmetric particles. In this context we mention the extension of continuum modelling of suspensions of swimming micro-organisms so as to enable the analysis of fully-developed bioconvection.

1. INTRODUCTION

Suspensions of dipolar particles appear in a wide variety of engineering applications (e.g. ferrofluids, cf. Rosensweig 1985) as well as natural phenomena (e.g. bioconvection set up by the swimming of certain micro-organisms, cf. Pedley & Kessler 1992). The macroscopic behaviour (i.e. rheology, transport phenomena, optical and electromagnetic properties, etc.) of such suspensions is substantially affected by the fact that, when subject to an appropriate external field, the suspended particles experience an orienting torque acting so as to align their dipole axis in the field direction. Thus, external magnetic fields influence the orientation of the single-domain, ferromagnetic particles suspended in a ferrofluid. Similarly, gravity affects the swimming direction of various species of algae possessing an asymmetric internal mass distribution, while certain bacteria contain magnetic particles and hence tend to move along magnetic field lines. All of the above orienting effects are collectively modelled by the response of a permanent dipole to an external field.

Calculation of the effective suspension properties involve ensemble averaging in which the orientational distribution density serves as the weight function [e.g. (1) *et seq.*]. The present analysis thus focuses on the calculation of this orientational distribution in a dilute suspension of Brownian axisymmetric dipolar particles in the limit of weak rotary diffusive effects.

The first analyses of the rheology of dilute suspensions of dipolar spheres were those of Hall & Busenberg (1969) and Brenner (1970b) who neglected the effect of rotary Brownian diffusion. This latter effect has been incorporated into the thorough study of Brenner & Weissman (1972). The limit of weak diffusion in the case when the deterministic particle rotary motion is periodic was discussed by Hinch & Leal (1972b). Shliomis (1972) studied the same problem by means of a 'relaxation equation' model. However, the latter is of rather *ad hoc* nature and is only applicable in certain limiting cases. Brenner & Weissman (1972) first suggested that the lack of agreement between their results and available experimental data regarding dipolar suspensions rheology was due to their disregard of the nonspherical shape of the suspended particles. Indeed, typical examples relevant to the manufacturing process of magnetic tapes and disks (Jhon et al. 1996) are single-domain rod-like $\gamma - Fe_2O_3$ particles and plate-like Ba-ferrite particles whose axis ratios are 7.5 and 0.1, respectively. Pedley & Kessler (1990) likewise mention as a typical example in the context of swimming micro-organisms prolate spheroidal cells of axis ratio about 1.4.

While the orientational distribution and rheology of dilute suspensions of torque-free nonspherical particles have extensively been studied (cf. the review by Brenner 1974), only a relatively few investigations considered dipolar nonspherical particles. Moreover, these are largely restricted to the limit of weak shear effects. Thus, Jansons (1983) calculated the bulk stress tensor for cases when the shear effect is small relative to the respective effects of both the external field and the rotary Brownian diffusion. Furthermore, some of the stress terms remained indeterminate since the orientational distribution was only calculated in the complete absence of shear. Pedley & Kessler (1990) obtained the first-order shear correction of the orientational distribution (relative to that pertaining to a quiescent fluid). Salueña et al. (1994) extended Jansons' (1983) analysis providing a higher-order term in the respective limits of weak shear and an external field which is either weak or strong relative to the rotary diffusive effects. Shear effects may, however, be quite significant. Thus, Smith & Bruce (1979) report experimental data regarding magnetic fluids at high shear rates corresponding to rotary Peclet numbers larger than 400. Similarly, Pedley & Kessler (1990) suggest that extension of the continuum theory of suspensions of micro-organisms to account for significant shear effect is an essential step towards the analysis of experimentally-observed fully-developed (nonlinear) collective motions.

An exception to the above is the numerical calculation of Strand & Kim (1992) who expanded the orientational distribution density into a series of surface harmonics and applied a Galerkin Method. However, their numerical scheme rapidly deteriorates with increasing value of the Langevin parameter due to poor convergence of the series expansion when steep gradients of the orientational distribution appear. Furthermore, physical insight into suspension macroscopic behaviour in the present singular limit of weak diffusion may only be obtained by relating the orientational distribution to the long-time limit of the corresponding deterministic motion (i.e. in the absence of diffusion) of the suspended particles. This requisite relation may not be inferred via some 'interpolation' between the cases of dipolar spheres and torque-free axisymmetric particles, since the motion of dipolar axisymmetric particles may be markedly different both quantitatively and qualitatively (cf. Almog & Frankel 1995). Owing to cumulative effects, even a weak external field or a small deviation from spherical shape may significantly modify the long-time limit of particle motion. Thus, unlike both of the above-mentioned problems, there are in the present problem cases when all particles approach a single stable limit cycle; in other cases multiple stable equilibrium orientations simultaneously

coexist and orientation space is accordingly divided into separate domains of attraction.

The rest of this contribution is arranged as follows. In the next section we briefly outline the main results of the general dynamic theory regarding the rheology of dilute suspensions, and formulate the boundary-value problem governing the steady orientational density distribution. The various asymptotic limits of this distribution are outlined in § 3. The results are then utilized to calculate the bulk stress which is discussed in § 4. In the concluding section we comment on the significance of the main results of the present contribution.

2. CALCULATION OF THE BULK STRESS

The dynamic theories of Batchelor (1970) and Brenner (1970a, 1972) provide a complete description of \mathbf{T} , the bulk (volume-averaged) stress in a dilute suspension (when hydrodynamic and other interparticle interactions are negligible). The dimensionless deviation of this bulk stress from the Newtonian stress

$$\frac{\mathbf{T} - 2\mu\mathbf{S}'}{\mu Gc} = 5 \langle \mathbf{A} \rangle - \frac{1}{2} \frac{Fr}{\mu G\tau_p} \boldsymbol{\epsilon} \cdot \langle \mathbf{L}^e \rangle \quad , \quad (1)$$

consists of symmetric and antisymmetric portions respectively represented by the terms on the right-hand side of (1). In this equation μ denotes the viscosity of the suspending fluid, \mathbf{S}' is the macroscopic rate-of-strain tensor (i.e., the symmetric portion of the bulk velocity gradient), c is the volume fraction of suspended particles, G is an appropriate norm [cf. (11)] of the bulk velocity gradient, $\boldsymbol{\epsilon}$ is the alternating isotropic third-rank pseudotensor, F is the magnitude of external field acting on the dipolar particles, r is the (permanent) dipole moment of a suspended particle, and τ_p its volume. The tensor \mathbf{A} and pseudovector \mathbf{L}^e respectively denote the dimensionless orientation-specific particle stress and external torque, and the symbol $\langle \rangle$ represents the corresponding orientational averages. For an axisymmetric particle whose orientation may effectively be represented by the unit vector \mathbf{e} attached to its axis of symmetry (see Fig. 1)

$$\langle \mathbf{x} \rangle \triangleq \int_{S_2} f(\mathbf{e}) \mathbf{x}(\mathbf{e}) d^2 \mathbf{e} \quad , \quad (2)$$

in which the weight function $f(\mathbf{e})$ is the steady long-time limit of the orientational density distribution to be discussed presently, and $d^2 \mathbf{e}$ is an areal element on S_2 , the surface of the unit sphere. Adapting the general expressions of Brenner (1972) to the present problem, we

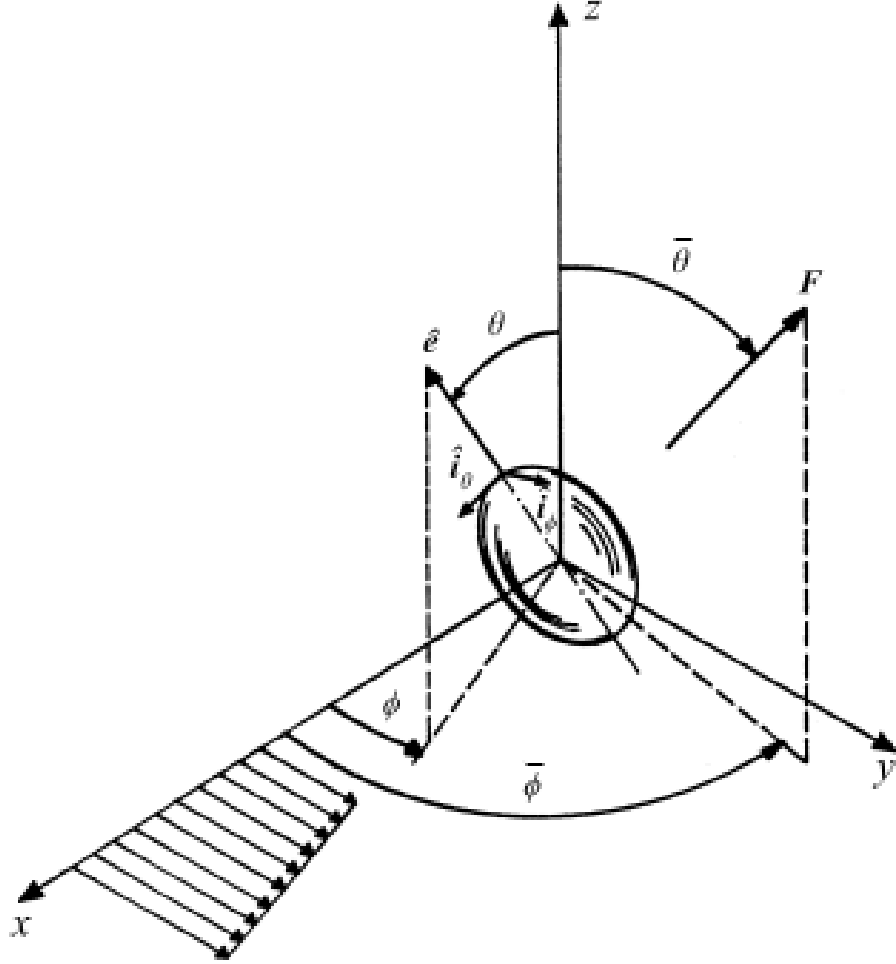


FIGURE 1. Definition of orientation $\mathbf{e} \equiv (\theta, \phi)$ of ax-symmetric particle suspended in simple shear flow (11) and subject to an external field acting in the direction $\hat{\mathbf{F}} \equiv (\bar{\theta}, \bar{\phi})$.

obtain

$$\begin{aligned} \langle \mathbf{A} \rangle = & \left(2N - \frac{3Q_{II}}{B} - \frac{4Q_{III}}{B} \right) \{ \langle \mathbf{ee} \rangle \cdot \boldsymbol{\Lambda} \}^s - 3Q_{II} \langle \mathbf{ee} \rangle \cdot \mathbf{S} + Q_{II} \mathbf{I} \langle \mathbf{ee} \rangle : \mathbf{S} \\ & - \left(\frac{3Q_{II}}{B} + \frac{4Q_{III}}{B} \right) \left\{ \lambda \left(\{ \langle \mathbf{e} \rangle \hat{\mathbf{F}} \}^s - \langle \mathbf{eee} \rangle \cdot \hat{\mathbf{F}} \right) + \frac{1}{\text{Pe}} (\mathbf{I} - 3 \langle \mathbf{ee} \rangle) \right\} + 2Q_I \mathbf{S} \quad , \quad (3) \end{aligned}$$

and

$$\langle \mathbf{L}^c \rangle = \langle \mathbf{e} \rangle \times \hat{\mathbf{F}} \quad . \quad (4)$$

In the above \mathbf{S} and \mathbf{A} are, respectively, the symmetric and antisymmetric portions of the bulk velocity gradient normalized with respect to G , $\{\}^s$ denotes the symmetrization operator, \mathbf{I} is the identity second-rank tensor, and the unit vector $\hat{\mathbf{F}}$ represents the direction of the external field. The parameters λ and Pe are defined later on. The scalars, Q_I, Q_{II}, Q_{III}, N , and B are intrinsic coefficients determined by particle geometry. (For spheroids these are known functions of the particle axis ratio, cf. Brenner 1974). Thus, once $f(\mathbf{e})$ is calculated, one may readily obtain the bulk stress by means of (1)-(4).

The steady orientational density distribution of dipolar axisymmetric particles which are uniformly distributed in physical space, $f(\mathbf{e})$, satisfies (cf. Brenner & Condiff 1974) the convection-diffusion equation

$$\text{Pe} \nabla_{\mathbf{e}} \cdot (\dot{\mathbf{e}} f) = \nabla_{\mathbf{e}}^2 f \quad (5)$$

The dimensionless time derivative of \mathbf{e} (normalized with respect to G) appearing in the convective term may be represented by the sum

$$\dot{\mathbf{e}} = \dot{\mathbf{e}}_1 + \lambda \dot{\mathbf{e}}_2 \quad , \quad (6a)$$

of the respective effects of shear

$$\dot{\mathbf{e}}_1 = \boldsymbol{\omega}_f \times \mathbf{e} + B(\mathbf{I} - \mathbf{e}\mathbf{e})\mathbf{e} : \mathbf{S} \quad , \quad (6b)$$

in which $\boldsymbol{\omega}_f$ is the (undisturbed) fluid angular velocity, and of \mathbf{L}^e , the orienting torque exerted on the dipolar particle by the external field \mathbf{F}

$$\dot{\mathbf{e}}_2 = \mathbf{L}^e \times \mathbf{e} = (\mathbf{I} - \mathbf{e}\mathbf{e}) \cdot \hat{\mathbf{F}} \quad . \quad (6c)$$

Equation (5) is supplemented by the normalization condition

$$\int_{S_2} f(\mathbf{e}) d^2\mathbf{e} = 1 \quad (7)$$

and the requirement that $f(\mathbf{e})$ be continuous and single-valued in S_2 . Appearing in the above are the rotary Peclet number

$$\text{Pe} = \frac{G}{d_r} \quad (8)$$

and the field parameter

$$\lambda = \frac{m_r Fr}{G} \quad (9)$$

wherein the scalar coefficients m_r and d_r are, respectively, the mobility and diffusivity corresponding to particle rotation about a transverse axis. The field parameter represents the relative effects of the external field and the shear flow on the rotary motion. For future reference it is also useful to define the Langevin parameter

$$\chi = \lambda \text{Pe} \quad (10)$$

representing the relative orienting and disorienting effects respectively associated with the external field and the rotary diffusion.

Obviously the bulk stress is a single-valued function of $(\chi, \text{Pe}, \bar{\mathbf{e}})$ inasmuch as, for a prescribed particle geometry and set of parameters, the steady orientational distribution employed in (2.1)-(2.4) is the unique long-time solution of the linear Fokker-Planck equation. The multiple-valued results presented by Rosensweig (1985, p. 267) thus essentially reflect the ad hoc nature of the relaxation equation from which they have been derived.

The present analysis focuses on the simple shear flow

$$\mathbf{u} = \hat{\mathbf{j}}Gx \quad (11)$$

wherein $(\hat{\mathbf{i}}, \hat{\mathbf{j}}, \hat{\mathbf{k}})$ is a right-handed triad of orthonormal space-fixed unit vectors in the directions of the (x, y, z) axes, and the scalar G denotes the shear rate. The analysis may be extended to a broader class of planar homogeneous shear flows through an appropriate reinterpretation of the parameters (cf. Hinch & Leal 1972a, Brenner 1974).

Parameterizing \mathbf{e} in terms of the polar angles (θ, ϕ) , the orientation-space gradient operator is

$$\nabla_{\mathbf{e}} = \hat{\mathbf{i}}_{\theta} \frac{\partial}{\partial \theta} + \hat{\mathbf{i}}_{\phi} \frac{1}{\sin \theta} \frac{\partial}{\partial \phi} \quad , \quad (12)$$

where $(\mathbf{e}, \hat{\mathbf{i}}_{\theta}, \hat{\mathbf{i}}_{\phi})$ is a right-handed triad of particle-fixed unit vectors (Fig. 1), and

$$\dot{\mathbf{e}} = \hat{\mathbf{i}}_{\theta} \dot{\theta} + \hat{\mathbf{i}}_{\phi} \dot{\phi} \sin \theta \quad . \quad (13)$$

Making use of these we obtain from (5)-(7)

$$\text{Pe} \left[\frac{\partial}{\partial \theta} (f \dot{\theta} \sin \theta) + \frac{\partial}{\partial \phi} (f \dot{\phi} \sin \theta) \right] = \frac{\partial}{\partial \theta} \left(\frac{\partial f}{\partial \theta} \sin \theta \right) + \frac{1}{\sin \theta} \frac{\partial^2 f}{\partial \phi^2} \quad , \quad (14)$$

$$\dot{\theta} = \frac{1}{4} B \sin 2\theta \sin 2\phi + \lambda [\sin \bar{\theta} \cos \theta \cos(\phi - \bar{\phi}) - \cos \bar{\theta} \sin \theta] \quad , \quad (15a)$$

$$\dot{\phi} = \frac{1}{2} (1 + B \cos 2\phi) - \lambda \frac{\sin \bar{\theta}}{\sin \theta} \sin(\phi - \bar{\phi}) \quad , \quad (15b)$$

and

$$\int_0^{\pi} \int_0^{2\pi} f \sin \theta d\phi d\theta = 1 \quad . \quad (16)$$

In (15a) and (15b) $\bar{\theta}$ and $\bar{\phi}$ are the polar angles characterizing $\hat{\mathbf{F}}$ (Fig. 1). It is worthwhile to mention that symmetry properties of (15a) and (15b) discussed by Almgog & Frankel (1995) allow us to restrict the variation of the parameters to the respective intervals $0 \leq \bar{\theta} \leq \pi/2$, $0 \leq \bar{\phi} \leq \pi$, and $0 \leq B \leq 1$.

Numerical solution of (14)-(16) has been obtained via a Galerkin method similar to that presented by Strand & Kim (1992): $f(\mathbf{e})$ is expanded in a series of surface spherical harmonics. Truncation of the series beyond the degree $n = N$ yields a system of $(N + 1)^2$ linear algebraic equations for the coefficients. The solution thus obtained approximates the projection of $f(\mathbf{e})$ onto the first N -harmonic subspace. In the next section we study the asymptotic behaviour of $f(\mathbf{e})$ in the limit when the effect of Brownian diffusion is weak relative to convection.

3. THE ORIENTATIONAL DISTRIBUTION

Before proceeding to the actual calculation of $f(\mathbf{e})$, we briefly discuss the dependence upon the parameters χ and Pe of the nature of prospective orientational distributions. A qualitative schematic description of the various domains in the plane of parameters (χ, Pe) is presented on a 'logarithmic' scale in Fig. 2 for $\bar{\theta} = \pi/2$. We primarily distinguish between two different limits:

- (1) Dominant diffusion when both $\chi, Pe \ll 1$. In this case (corresponding to the bottom left portion of the figure), we anticipate a nearly uniform orientational distribution. The first-order deviation from such uniform distribution is expressible as a superposition of correction terms corresponding to the respective effects of fluid shear and external field. These, in turn, have previously been obtained by Brenner & Condiff (1972,1974).
- (2) Weak diffusion when $\chi \gg 1$ or $Pe \gg 1$. We expect the orientational distribution in this case to be closely related to the long-time behaviour of the corresponding deterministic rotary motion (i.e., for the same λ and $\hat{\mathbf{F}}$ in the absence of Brownian diffusion). With a few exceptions (cf. Almog & Frankel 1995), in the latter problem as $t \rightarrow \infty$ the dipolar particles approach either a stable equilibrium orientation or a stable limit cycle. Whether or not the resulting orientational distribution is of boundary-layer type depends, however, on the strength of the corresponding attractor. In order to clarify this point we compare $(d_r)^{-1}$, the diffusive time scale, and the characteristic time associated with the deterministic rotary motion in the limit $\lambda \ll 1$. According to Almog & Frankel (1995), the latter is $O(1/\lambda^2 G)$ when the external field acts in the plane of shear ($\bar{\theta} = \pi/2$) and $O(1/\lambda G)$ when the field has a nonzero component in the direction of the undisturbed fluid vorticity ($\bar{\theta} \neq \pi/2$). Both (diffusive- and convective-) time scales will

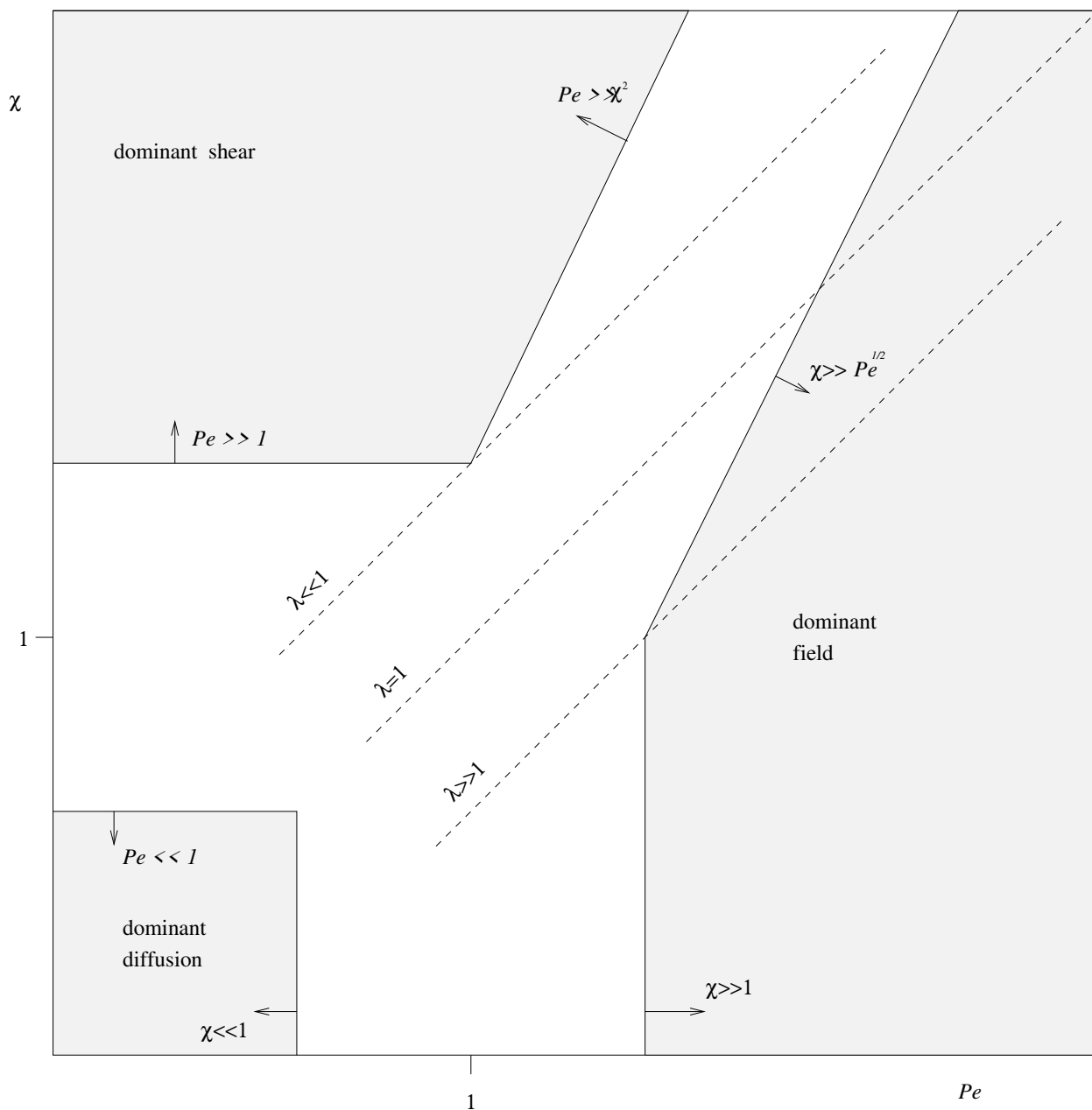


FIGURE 2. Schematic description of the various domains in the plane of parameters (χ, Pe) for an external field acting in the plane of shear $\theta = \pi/2$.

thus be comparable for $\chi \sim O(\text{Pe}^{1/2})$ when $\bar{\theta} = \pi/2$ and for $\chi \sim O(1)$ otherwise.

We conclude that for fixed $\text{Pe} \gg 1$ and sufficiently small λ , rotary diffusion, though weak, will have a global effect throughout S_2 . Indeed, asymptotic calculation in the domain of 'dominant shear' (indicated at the upper left of Fig. 2, cf. § 3.2) yields a rather even orientational distribution as opposed to the boundary-layer type distributions obtained for sufficiently large values of λ (at the right of the figure). When $\bar{\theta} \neq \pi/2$ some changes take place in the location of the boundaries of the respective domains of dominant external field and dominant shear. (Thus, for instance, in agreement with the above estimates, orientational boundary-layer distributions may occur whenever $\chi \gg 1$.) This may result in some overlap between the various domains of weak diffusion, thereby allowing for a smooth transition between the corresponding asymptotic solutions for the orientational distribution (cf. § 3.2).

3.1. Boundary-layer distributions.

3.1.1. *A Stable equilibrium orientation.* As established by Almgog & Frankel (1995) and mentioned above, for sufficiently large values of λ , the dipolar particles approach, in the absence of Brownian diffusion, a stable equilibrium orientation. Large gradients of $f(\mathbf{e})$ are expected in the immediate vicinity of this orientation and diffusive effects will no longer be negligible there. We thus seek a boundary-layer-type orientational distribution. Define the 'inner' coordinates

$$\theta = \theta_c + \delta\alpha, \quad \text{and} \quad \phi = \phi_c + \epsilon\beta \quad (3.17\text{a,b})$$

where $\mathbf{e}_c \equiv (\theta_c, \phi_c)$, the equilibrium orientation, is obtained by setting $\dot{\mathbf{e}} = 0$ in (6a) and (6b) and $\epsilon, \delta \rightarrow 0$ as $\text{Pe}, \chi \rightarrow \infty$. The respective effects of diffusion and external field balance within the boundary layer for

$$\delta = \chi^{-1/2}, \quad \text{and} \quad \epsilon = \chi^{-1/2} / \sin \theta_c. \quad (3.18\text{a,b})$$

(Thus an expansion about $(\bar{\theta}, \bar{\phi})$ rather than (θ_c, ϕ_c) will be nonuniform unless the displacement of \mathbf{e}_c from $\hat{\mathbf{F}}$, which for large λ is $O(\lambda^{-1})$, is smaller than the boundary-layer thickness, i.e. unless $\chi \gg \text{Pe}^2$. Furthermore, some minor modifications are required when $\bar{\theta} = 0$, because $\theta_c = 0$ then.) Expanding (14), (15a) and (15b) in terms of these inner

variables yields

$$f \cong \frac{\chi}{2\pi} (C_1 C_3 - C_2^2)^{1/2} \exp \left[-\frac{1}{2} (C_1 \alpha^2 + 2C_2 \alpha \beta + C_3 \beta^2) \right] [1 + \chi^{-1/2} f_1(\alpha, \beta) + O(\chi^{-1})], \quad (3.19a)$$

up to and including a first-order $O(\chi^{-1/2})$ correction (which is not explicitly presented here). The above solution is only valid provided that the constants C_1, C_2, C_3 (which, in turn, depend upon a_{ij} ($i, j = 1, 2$), the scalar components of $\nabla_e \dot{e}$) satisfy $C_1 C_3 - C_2^2 > 0$. It is easy to show that the latter inequality is equivalent to the requirement that \mathbf{e}_c be a stable equilibrium orientation. In the particular case when $\bar{\theta} = \pi/2$ we have

$$f \cong \frac{\chi}{2\pi} (a_{11} a_{22})^{1/2} \exp \left[-\frac{1}{2} (a_{11} \alpha^2 + a_{22} \beta^2) \right] [1 + \chi^{-1/2} f_1(\alpha, \beta) + O(\chi^{-1})]. \quad (3.19b)$$

It is worthwhile to emphasize that, unlike earlier weak-shear approximations in the literature, validity of the present results does not require that $\text{Pe} \ll 1$ nor in fact even $\text{Pe} \ll \chi$. Rather, (3.19a) and (3.19b) are valid provided that the stable node at \mathbf{e}_c be sufficiently attractive so that the coefficients a_{ij} are $O(1)$. This is satisfied for large enough $\lambda \sim O(1)$ (cf. the discussion of Fig. 3). Finally, the above calculation tacitly assumes that \mathbf{e}_c is the unique stable equilibrium orientation. The analysis may in principle be extended to the case when there simultaneously coexist more than one such orientation. The orientational distribution may then be obtained via superposition provided that the normalization condition is modified so as to allocate the appropriate relative weight to each of the stable equilibrium points.

3.1.2. A stable limit cycle. A stable limit cycle may exist in the deterministic problem when the external field is nearly parallel to the plane of shear (i.e. $\cos \bar{\theta} \ll 1$) and acts in an azimuthal direction $0 < \bar{\phi} < \pi/2$ (Almog & Frankel 1995). We focus here on the case $\bar{\theta} = \pi/2$ when the limit cycle coincides with the unit circle $\theta = \pi/2$. Define the inner variable α via

$$\theta = \pi/2 + \text{Pe}^{-1/2} \alpha \quad . \quad (3.20)$$

From (14), (15a), and (15b) together with the requirement of periodicity $f(\alpha, \phi + 2\pi) = f(\alpha, \phi)$, we obtain

$$f(\alpha, \phi) \cong A \text{Pe}^{1/2} \left[2\pi \dot{\phi}_0 (\Delta(\phi))^{1/2} \right]^{-1} \exp \left[-\frac{\alpha^2}{4\Delta(\phi)} \right] [1 + O(\text{Pe}^{-1})] \quad , \quad (3.21)$$

in which the $O(1)$ coefficient A is obtainable from the normalization condition (16). The various functions of ϕ appearing in (3.21) are

$$\dot{\phi}_0(\phi) = \dot{\phi} \Big|_{\theta=\pi/2} \quad , \quad \dot{\theta}_1(\phi) = \frac{\partial \dot{\theta}}{\partial \theta} \Big|_{\theta=\pi/2} \quad , \quad (3.22a,b)$$

$$F(\phi) \triangleq - \int_0^\phi \frac{\dot{\theta}_1(\varphi)}{\dot{\phi}_0(\varphi)} d\varphi \quad (3.22c)$$

$$G(\phi) \triangleq e^{-2F(\phi)} \int_0^\phi \frac{e^{2F(\varphi)}}{\dot{\phi}_0(\varphi)} d\varphi \quad , \quad \Delta(\phi) \triangleq G(\phi) + G(2\pi) \frac{e^{-2F(\phi)}}{1 - e^{-2F(\phi)}} \quad . \quad (3.22d,e)$$

The first-order $O(\text{Pe}^{-1})$ correction to f (which is not explicitly presented in (3.5)) has been obtained as well and is utilized in the next section. When a stable limit cycle exists, $\dot{\phi}_0 > 0$ for all ϕ . From the definition (3.22c) of $F(\phi)$, $F(2\pi)$ is related to the increment in θ along a segment of (deterministic) particle path between $\phi = 0$ and $\phi = 2\pi$. From this kinematic interpretation together with the assumed stability of the limit cycle there immediately follows the inequality $F(2\pi) > 0$. Thus, by (3.22d,e) $\Delta(\phi) > 0$ which, in turn, is necessary for the validity of (3.21).

The above results allow for the simple qualitative interpretation of the distribution about a stable limit cycle as the product of a quasi one-dimensional Gaussian distribution in the $\hat{\mathbf{i}}_\theta$ direction (whose 'local' width is determined by the local attraction $\Delta^{-1}(\phi)$) multiplied by $\dot{\phi}_0^{-1}$ representing the relative residence time of the particle at the orientation ϕ along the limit cycle.

Uniformity of the foregoing boundary-layer approximation may be restricted to a relatively narrow interval of λ (cf. Fig. 7). With decreasing λ , $F(2\pi)$ and $\Delta(\phi)$ decrease as a result of the diminishing attraction of the limit cycle in the deterministic problem. Thus, contrary to the assumption underlying the present derivation, f (3.21) no longer represents (the leading behaviour of) a narrow boundary layer centred about the limit cycle. With increasing λ , the corresponding deterministic problem undergoes a bifurcation which changes the nature of the attractor. A stable node appears on $\theta = \pi/2$ at which point $\dot{\phi}_0$ vanishes and f turns singular. The transition in the nature of the orientational distribution accompanying the bifurcation of the deterministic problem is examined next.

3.1.3. *A saddle-node point.* We seek to approximate the orientational distribution for $\bar{\theta} = \pi/2$ and $0 < \bar{\phi} < \pi/2$ when

$$\lambda = \lambda_b(\bar{\phi}, B) + \nu\lambda_1, \quad (3.23)$$

in which $\lambda_b(\bar{\phi}, B)$ corresponds to the bifurcation when, in the absence of Brownian diffusion, the attracting set changes from a limit cycle for $\lambda < \lambda_b$ to a stable node for $\lambda > \lambda_b$. At the saddle-node point $\mathbf{e}_b = (\pi/2, \phi_b)$ $\dot{\theta} = \dot{\phi} = 0$ and $\left. \partial\dot{\phi}/\partial\phi \right|_b = 0$, i.e. the eigenvalue of $\nabla_{\mathbf{e}} \dot{\mathbf{e}}$ corresponding to the eigenvector $\hat{\mathbf{i}}_{\phi}$ vanishes. We further assume that the saddle-node point is sufficiently attractive in the $\hat{\mathbf{i}}_{\theta}$ direction, i.e.

$$a \triangleq - \left. \frac{\partial\dot{\theta}}{\partial\theta} \right|_b > 0 \quad (3.24)$$

is $O(1)$. From the boundary-layer solutions of the preceding subsections we anticipate that when $|\lambda - \lambda_b| \ll 1$ the distribution will effectively be concentrated about the saddle-node. We thus introduce the boundary-layer coordinates

$$\theta = \pi/2 + \delta\alpha, \quad \text{and} \quad \phi = \phi_c + \epsilon\beta. \quad (3.25a,b)$$

Expanding (14), (15a), and (15b) in terms of these coordinates we obtain the order estimates: (i) $O(\text{Pe})$ for convective terms associated with $\dot{\theta}$, (ii) $O(\delta^{-2})$ for diffusive terms resulting from gradients with respect to θ , (iii) $O(\text{Pe}\epsilon, \text{Pe}\delta^2/\epsilon, \text{Pe}\nu/\epsilon)$ for convection in the $\hat{\mathbf{i}}_{\phi}$ direction, and (iv) $O(\epsilon^{-2})$ for diffusion in the $\hat{\mathbf{i}}_{\phi}$ direction. The present limit is expected to be intermediate between the previously analysed cases. We therefore anticipate the decay of $f(\mathbf{e})$ to be slower in the $\hat{\mathbf{i}}_{\phi}$ direction, i.e. $\delta \ll \epsilon$. Furthermore, unlike the expansion near a limit cycle where diffusion associated with azimuthal density gradients was negligible, we expect here diffusive and convective terms in the azimuthal direction to be of the same order. Similarly to previous boundary-layer solutions, diffusion and convection in the $\hat{\mathbf{i}}_{\theta}$ direction are expected to balance each other in the leading order. The foregoing considerations lead to the scaling

$$\delta = \text{Pe}^{-1/2}, \quad \epsilon = \text{Pe}^{-1/3} \quad (3.26a,b)$$

and therefore

$$\nu = \epsilon^2 = \text{Pe}^{-2/3}. \quad (3.26c)$$

It is worthwhile to note that the stable node (at ϕ_c) occurring when $\lambda_1 > 0$ is displaced from the saddle-node point by $|\phi_c - \phi_b| \sim O(\nu^{1/2})$. Thus, the latter relation serves to insure that the critical point is located within the inner domain of the present expansion.

In terms of the inner variables, the leading-order problem yields

$$f \cong A \text{Pe}^{5/6} h(\beta) \exp \left\{ -\frac{1}{2} a \alpha^2 \right\} [1 + O(\epsilon)] \quad (3.27)$$

wherein the $O(1)$ constant A is obtainable from the normalization condition and $h(\beta)$ is an arbitrary function of β . The latter is calculated from a solvability condition in the next-order balance which yields

$$h(\beta) = \exp \left(\frac{1}{3} b \beta^3 + b_0 \lambda_1 \beta \right) \int_{\beta}^{\infty} \exp \left(-\frac{1}{3} b \beta_1^3 - b_0 \lambda_1 \beta_1 \right) d\beta_1 \quad . \quad (3.28)$$

In (3.28) appear the constant coefficients

$$b_0 \triangleq \left. \frac{\partial \dot{\phi}}{\partial \lambda} \right|_b < 0 \quad , \quad \text{and} \quad b \triangleq \left. \frac{\partial^2 \dot{\phi}}{\partial \phi^2} \right|_b > 0$$

whose respective signs may be ascertained by considering the details of the deterministic motion for $\lambda \approx \lambda_b$. The function $h(\beta)$ decays like $O(\beta^{-2})$ for $|\beta| \gg 1$, and at the bifurcation it is

$$h = e^{\frac{1}{3} b \beta^3} \Gamma \left(\frac{1}{3}, \frac{1}{3} b \beta^3 \right) \quad . \quad (3.29)$$

Employing Laplace's method one may verify that (3.27) becomes equivalent to the respective leading orders of (3.19b) and (3.21) when $\lambda_1 \rightarrow \pm\infty$. It is thus demonstrated that the present inner solution about a saddle-node point indeed describes the transition from a boundary layer about a limit cycle (for $\lambda_1 \rightarrow -\infty$) to a boundary-layer distribution about a stable equilibrium orientation (when $\lambda_1 \rightarrow \infty$).

Finally, it is interesting to note that, unlike the exponentially decaying boundary-layer expansions obtained in the preceding subsections, consistent calculation of a correction term (which is omitted here) requires in the present case the consideration of a non-trivial outer solution.

3.2. Dominant shear. We now consider the case when $\text{Pe} \gg 1$ and $\lambda \ll 1$. (It is worthwhile to mention that when $\bar{\theta} \neq \pi/2$, even the simpler problem for a dipolar sphere has not previously been solved.) According to the discussion at the beginning of this section, the (weak) influence of rotary diffusion is not necessarily confined to narrow orientational boundary layers but may rather have a global effect on the orientational distribution. From (5) we obtain the leading-order equation

$$\nabla_e \cdot (\dot{e}_1 f) = 0 \quad (3.30)$$

whose characteristic curves are the family of closed Jeffery orbits (Jeffery 1922). Following Leal & Hinch (1971), we introduce the transformation

$$\tan \phi = R \tan \tau \quad , \quad \text{and} \quad \tan \theta = C(R^2 \sin^2 \tau + \cos^2 \tau)^{1/2} \quad (3.31a,b)$$

from the polar angles to the 'natural' coordinates C , the orbit parameter (denoting a specific orbit), and τ , the phase along the orbit. In the above $R = [(1+B)/(1-B)]^{1/2}$ is the effective axis ratio of the axisymmetric particle.

The solution of (3.30) is rendered unique by a method originally proposed by Batchelor (1956) in the context of closed-streamline flow fields at large Reynolds numbers and later applied by Leal & Hinch (1971) in obtaining the steady, large-Peclet-number orientational distribution in the absence of external field ($\lambda = 0$). To this end, we integrate (5) over a domain in S_2 bounded by a single Jeffery orbit ($C=\text{const.}$). Making use of the divergence theorem we arrive at

$$\oint_{C=\text{const.}} \frac{\partial f}{\partial n} dl = \chi \oint_{C=\text{const.}} (\hat{\mathbf{n}} \cdot \dot{\mathbf{e}}_2) f dl \quad , \quad (3.32)$$

in which $\hat{\mathbf{n}}$ is an outwardly directed unit vector normal to the integration contour and lying in S_2 . The resulting condition expresses the vanishing at steady state of the net rotary flux induced by both diffusion and external field across the Jeffery orbit $C=\text{const.}$.

Expressing (3.30) in terms of the natural coordinates (C, τ) the resulting equation is readily integrated to yield

$$f = F(C)g(C, \tau) \quad , \quad (3.33)$$

where

$$g(C, \tau) \triangleq \left(\frac{\partial(\theta, \phi)}{\partial(C, \tau)} \sin \theta \right)^{-1} .$$

Substituting (3.33) into (3.32) we obtain a first-order equation for $F(C)$ which yields

$$F(C) = AF^0(C) \exp \left[-\frac{4\chi}{\pi} \cos \bar{\theta} h(C) \right] \quad (3.34)$$

where $F^0(C) = F(C)|_{\chi=0}$ (cf. Leal & Hinch 1971), and

$$h(C) = \begin{cases} \int_0^C \mathfrak{H}(C_1) dC_1 & C > 0 \\ \int_{-\infty}^C \mathfrak{H}(C_1) dC_1 + \int_0^{\infty} \mathfrak{H}(C_1) dC_1 & C < 0 \end{cases} ,$$

in which

$$\mathfrak{H}(C) \triangleq \frac{|C|(1+C^2R^2)^{1/2} E \left(\frac{C^2(R^2-1)}{1+C^2R^2} \right)}{HC^4 + KC^2 + M} \quad ,$$

$E(\cdot)$ denoting the complete elliptic integral of the second kind. The constant coefficient A is calculated from the normalization condition. The R -dependent coefficients $H(R)$, $K(R)$, and $M(R)$ are tabulated by Leal & Hinch (1971).

From (3.34) we see that, in the present limit, the external field affects the leading order of the orientational distribution only through the appearance of $\chi \cos \bar{\theta}$ in the exponential factor. Thus, when $\bar{\theta} = \pi/2$ f is the same as the one obtained by Leal & Hinch (1971) in the absence of external field. On the other hand, when $0 \leq \bar{\theta} < \pi/2$ and $1 \ll \chi \cos \bar{\theta} (\ll \text{Pe})$, f becomes increasingly concentrated about $C = 0$ (i.e. $\theta = 0$) which, in turn, minimizes $h(C)$. (Cf. (3.31a,b) and the above definitions of $h(C)$ and $\mathfrak{H}(C)$.) These results may be rationalized in terms of the nearly periodic deterministic motion under the action of a weak ($\lambda \ll 1$) external field. In this context, Almog & Frankel (1995) noted that no net rotary flux across Jeffery orbits is induced by the external field acting in the plane of shear ($\theta = \bar{\pi}/2$). However, when $0 \leq \bar{\theta} < \pi/2$ a stable spiral point exists at $\theta_c \sim O(\lambda)$ (irrespective of the azimuthal direction $\bar{\phi}$) and the external field thus generates a drift of the particles across Jeffery orbits towards $\theta = 0$. With increasing intensity of the external field we therefore anticipate a gradual transformation of f from an even distribution over the family of Jeffery orbits to an orientational boundary layer about the stable (spiral) critical point. In accordance with Fig. 2 and the accompanying discussion, no such smooth transition of the orientational distribution is expected when $\bar{\theta} = \pi/2$.

Finally, from the calculation of the correction term (which is omitted here), one concludes that the correction associated with the external field (which for $\chi \gg 1$ is the dominant correction) is $O(\chi^3/\text{Pe})$ for $\bar{\theta} \neq \pi/2$ and $O(\chi^2/\text{Pe})$ for $\bar{\theta} = \pi/2$. The latter estimate is the basis for defining the boundary of the 'dominant shear' domain presented in Fig. 2, so as to insure that the present expansion is indeed asymptotic throughout that domain. The resulting schematic description is thus in agreement with the prediction of no overlap of the domains of dominance of shear and external field, respectively. The above estimates together with the discussion at the very beginning of § 3 indicate, however, that such an overlap does exist when $\bar{\theta} \neq \pi/2$ and $1 \ll \chi \ll \text{Pe}^{1/3}$, which supports the earlier discussion of (3.34).

4. RESULTS AND DISCUSSION

In the following we make use of the above outlined results regarding the orientational distribution to calculate the suspension bulk stress.

We here focus on the case $\bar{\theta} = \pi/2$ (external field acting in the plane of shear), when the particles contribution to the bulk stress is planar and is completely specified [cf. (1)] in terms of the intrinsic viscosity

$$[\eta] \triangleq \frac{\frac{1}{2}(T_{12} + T_{21}) - 2\mu S_{12}}{\mu Gc} = 5 \langle A_{12} \rangle \quad , \quad (4.35a)$$

the normal-stress differences

$$[\tau_1] \triangleq \frac{T_{11} - T_{33}}{\mu Gc} = 5(\langle A_{11} \rangle - \langle A_{33} \rangle), \quad \text{and} \quad [\tau_2] \triangleq \frac{T_{22} - T_{33}}{\mu Gc} = 5(\langle A_{22} \rangle - \langle A_{33} \rangle) \quad , \quad (4.35b, c)$$

describing $\langle \mathbf{A} \rangle$, the deviatoric particle stress, and

$$[\tau^a] \triangleq \frac{T_{12} - T_{21}}{2\mu Gc} = -\frac{1}{2} \frac{Fr}{\mu G\tau_p} \langle L_3^e \rangle \quad , \quad (4.35d)$$

representing the average external couple. In accordance with the calculations of the preceding section which focused on the limit of weak diffusion, most subsequent results describe the variation with λ , the field parameter (9), and $\bar{\phi}$, the azimuthal direction of the external field, of the planar bulk stress at large Peclet numbers, $Pe \gg 1$. When a single stable equilibrium orientation \mathbf{e}_c exists, and for sufficiently large $\chi \gg 1$, the boundary layer about \mathbf{e}_c becomes so narrow that one anticipates the goniometric factors occurring in (3) and (4) to be approximately $\langle \mathbf{e} \rangle \cong \mathbf{e}_c$, $\langle \mathbf{e}\mathbf{e} \rangle \cong \mathbf{e}\mathbf{e}_c, \dots$, etc. Making use of the boundary-layer approximation (3.19b) we obtain

$$\frac{1}{5}[\eta] \cong \frac{1}{4}(3Q_{II} + 4Q_{III}) \cos^2 2\phi_c + \frac{1}{2}N \cos 2\phi_c - \frac{3}{4}Q_{II} + Q_I + \chi^{-1}[\eta^{(2)}] + O(\chi^{-3/2}) \quad , \quad (4.36a)$$

$$\frac{1}{5}[\tau_1] \cong -\frac{1}{4}(3Q_{II} + 4Q_{III}) \sin 2\phi_c \cos 2\phi_c - \left(\frac{1}{2}N + \frac{3}{4}Q_{II} \right) \sin 2\phi_c + \chi^{-1}[\tau_1^{(2)}] + O(\chi^{-3/2}) \quad , \quad (4.36b)$$

$$\frac{1}{5}[\tau_2] \cong \frac{1}{4}(3Q_{II} + 4Q_{III}) \sin 2\phi_c \cos 2\phi_c + \left(\frac{1}{2}N - \frac{3}{4}Q_{II} \right) \sin 2\phi_c + \chi^{-1}[\tau_2^{(2)}] + O(\chi^{-3/2}) \quad , \quad (4.36c)$$

and

$$[\tau^a] \cong \frac{3}{2}K_r(1 + B \cos 2\phi_c) + \chi^{-1}(\tau^a)^{(2)} + O(\chi^{-3/2}) \quad , \quad (4.36d)$$

correct to $O(\chi^{-1})$ terms ¹(which are not explicitly presented here). In (4.36d) $K_r = (6\mu\tau_p m_r)^{-1}$ denotes the intrinsic hydrodynamic resistance to rotation of the particle about a transverse axis. These asymptotic results show that the respective leading-order terms indeed depend upon ϕ_c alone.

Figure 3 presents the variation of $[\eta]$ with λ for a prolate spheroid ($R = 3$) at $\text{Pe} = 100$ and $\bar{\phi}/\pi = 0$ (a) $1/4$ (b), $5/12$ (c), $1/2$ (d), $7/12$ (e), $2/3$ (f), $5/6$ (g), and 1 (h). Solid lines represent exact results obtained via the numerical scheme mentioned at the conclusion of § 2. [In fact, the evaluation of the goniometric factors $\langle \mathbf{e} \rangle$, $\langle \mathbf{e}\mathbf{e} \rangle$, \dots , etc. involved in the calculation of the bulk stress only requires a few coefficients of the lowest-order surface harmonics in the expansion of $f(\mathbf{e})$]. The dotted lines are based on the boundary-layer approximation (4.36a). In all cases presented (except for $\bar{\phi} = \pi/2$, $7\pi/12$ which are discussed later on) the exact results are indistinguishable from the latter approximation for $\lambda \gtrsim 0.5$. In the following we take advantage of this agreement and present only (4.36a) for $\lambda > 1$ where performance of the numerical scheme deteriorates (cf. Strand & Kim 1992).

A common feature in all parts of the figure is that $[\eta]$ is nearly constant up to $\lambda \cong 0.1$. This observation accords with the asymptotic results (3.34) indicating that, for an external field acting in the plane of shear ($\bar{\theta} = \pi/2$), λ does not affect the leading order of the orientational distribution. Other than this, the variation of $[\eta]$ with λ appears both quantitatively and qualitatively different for the different values of $\bar{\phi}$. However, by (4.36a)-(4.36d) for χ sufficiently large the bulk stress depends upon $\bar{\phi}$ and λ only through their combination in ϕ_c (rather than on each parameter separately). This suggests a unified manner of description of the different modes of variation as well as a mechanistic explanation of the various trends appearing in the preceding figure.

Accordingly, Fig. 4 presents the variation of $[\eta]$ with ϕ_c at $\text{Pe} = 100$ for a prolate spheroid whose axis ratio is $R = 3$. The bold solid curves represent $\bar{\phi} = 0, \pi/2$ and $2\pi/3$ and the dotted line $\bar{\phi} = 7\pi/12$ (respectively corresponding to parts (a), (d), (f), and (e) of Fig. 3). The thin solid line describes the variation of $[\eta]$ in the limit of $\text{Pe} \rightarrow \infty$ and fixed $\lambda \sim O(1)$ according to (4.36a). For each value of $\bar{\phi}$, ϕ_c is uniquely determined by λ (Almog & Frankel 1995), and is monotonically decreasing with λ towards the limit $\phi_c = \bar{\phi}$ as $\lambda \rightarrow \infty$. (Thus the parameter λ increases leftwards along each of the curves.)

¹Making use of the $O(\chi^{-1})$ term in the normalization condition (7), one readily verifies that, the second-order correction in (3.3b) will only affect $O(\chi^{-3/2})$ terms in the goniometric factors.

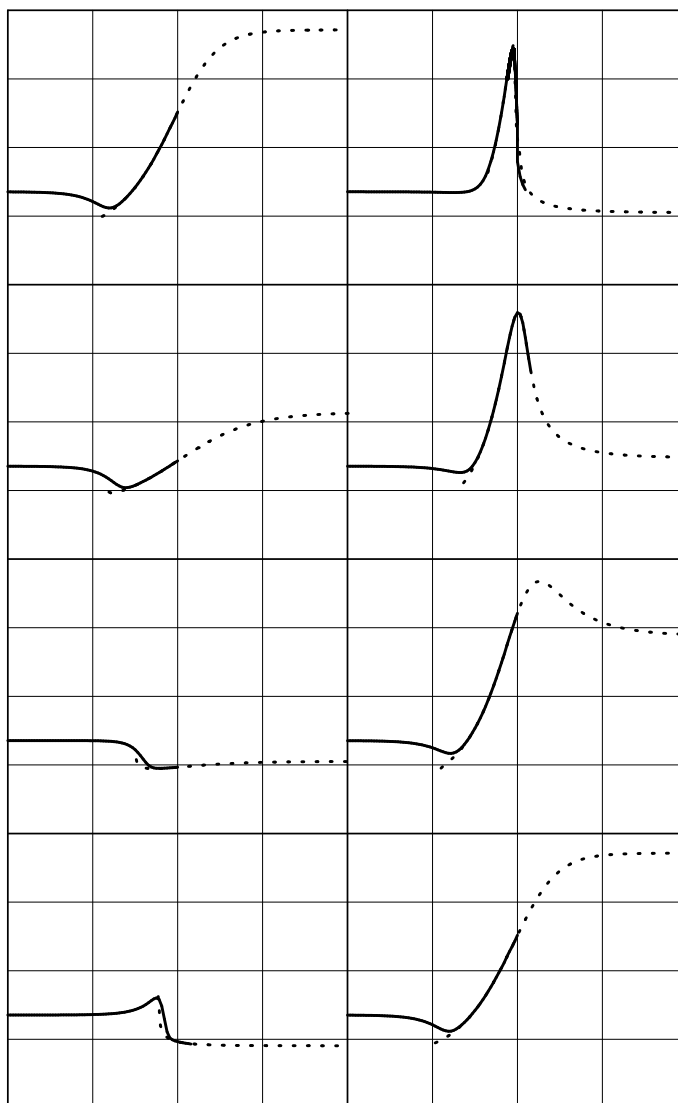


FIGURE 3. Variation of $[\eta]$, the intrinsic viscosity, with λ for a suspension of prolate spheroids ($R = 3$) at $Pe = 100$, $\bar{\theta} = \pi/2$ and azimuthal directions of external field $\bar{\phi}/\pi = 0$ (a), $1/4$ (b), $5/12$ (c), $1/2$ (d), $7/12$ (e), $2/3$ (f), $5/6$ (g), and 1 (h). — exact (numerical) results, boundary-layer approximation (4.36a).

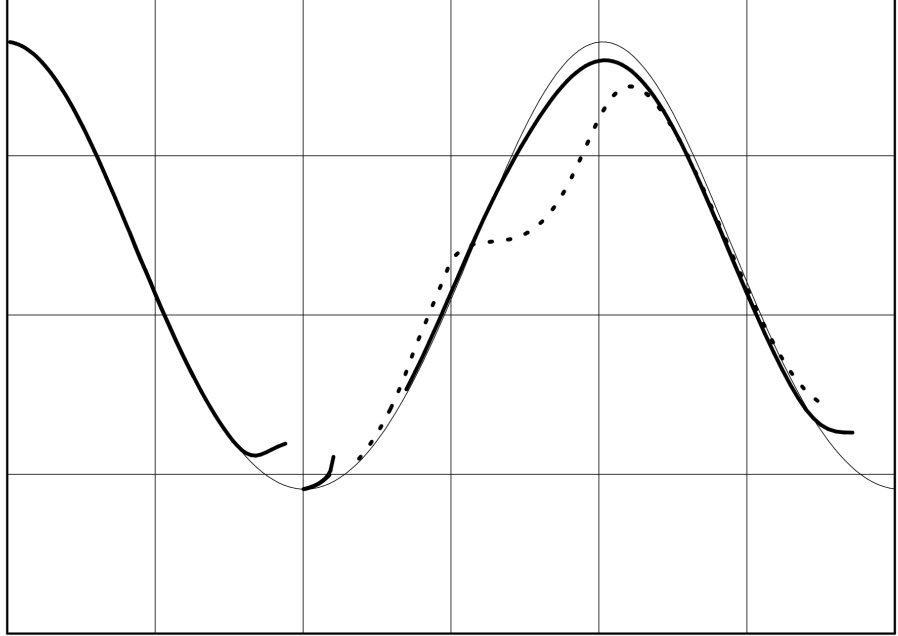


FIGURE 4. Variation of $[\eta]$, with ϕ_c , the azimuthal direction of (deterministic) stable equilibrium orientation, for a suspension of prolate spheroids ($R = 3$) at $Pe = 100$ and the indicated azimuthal directions of external field (bold solid or dotted lines). Thin solid curve represents the leading order behaviour in (4.36a).

The curves pertaining to $\bar{\phi} = 0$ and $2\pi/3$, (and indeed all other values of $\bar{\phi}$ appearing in Fig. 3 and not presented here) show for sufficiently large ($\sim O(1)$) λ a remarkable agreement with the universal asymptote based on the leading-order term of (4.36a). This latter term reflects the relation between the rate of dissipation and particles orientation: When the (prolate) particles align with the streamlines ($\phi_c = \pi/2$ in the present problem), the rate of dissipation is minimized; it is maximized when the particles are oriented perpendicularly to the undisturbed fluid velocity ($\phi_c = 0$). The trends observed earlier in Fig. 3 may now be rationalized via comparison of the various curves there to their counterparts here. It thus becomes clear that for $\bar{\phi} = 0$ and λ sufficiently large (to insure validity of the boundary-layer approximation),

$[\eta]$ monotonically increases towards its absolute (i.e. for all λ and $\bar{\phi}$ at $Pe \gg 1$) maximal value which is attained in the limit $\lambda \rightarrow \infty$ when $\phi_c \rightarrow \bar{\phi}=0$. Similarly, for $\bar{\phi} = 2\pi/3$, $[\eta]$ initially increases to a maximal value when $\phi_c = \pi$ (which local maximum is slightly lower than the former absolute maximum because it is attained when $\lambda \cong 1$ and the boundary layer is not yet sufficiently narrow to insure that all particles effectively share the equilibrium orientation $\phi_c = \pi$). With further increase in λ , ϕ_c continues to decrease towards the limit $\phi_c = \bar{\phi} = 2\pi/3$ for $\lambda \rightarrow \infty$ and $[\eta]$ accordingly decreases as well.

As mentioned before, the behaviour of the curves corresponding to $\bar{\phi} = \pi/2, 7\pi/12$ is exceptional. When $\bar{\phi} = \pi/2$ matching of the exact (numerical) and approximate (boundary-layer) solution in Fig. 3(d) is only achieved at relatively large values of $\lambda (> \sim 1)$ and then only over a relatively narrow interval of ϕ_c in Fig. 4. For $\bar{\phi} = 7\pi/12$, contrary to all other curves presented, which monotonically approach the boundary-layer asymptote with $\lambda (> \sim 0.5)$, here when $\lambda \cong 1$, the $[\eta]$ curve (in both Fig. 3(e) and Fig. 4) substantially deviates from the asymptote, rejoining it only at larger values of λ . These peculiarities may be rationalized in terms of the corresponding deterministic particle motion. Thus (cf. Almog & Frankel 1995) when $\bar{\phi} = \pi/2$ and $\lambda < 0.9$ a certain part of orientation space is spanned by a family of closed orbits. Attraction to the stable equilibrium orientation is confined to the rest of orientation space. In the case of $\bar{\phi} = 7\pi/12$, when $\lambda \cong 1$ the curve corresponding to $\dot{\phi} = 0$ in the deterministic problem is nearly tangent to the circle $\theta = \pi/2$. As a result $\left(\partial\dot{\phi}/\partial\phi\right)_c$, the eigenvalue of $\nabla_e \dot{e}|_{e_c}$ corresponding to the azimuthal direction [cf. (3.23) *et seq.*] nearly vanishes [see Fig. 5(a)]. Thus, despite the relatively large value of λ , the equilibrium orientation is locally (for this value of λ) insufficiently stable to insure the existence of a boundary-layer distribution. Another result of the tangency mentioned above is the steep decrease of ϕ_c with λ which may be observed in Fig. 5(b). This in turn explains the abrupt changes of $[\eta]$ with $\lambda \cong 1$ in Fig. 3(e).

For the specific shape selected in the present illustration (i.e. $R = 3$), the values $\bar{\phi} = \pi/2, \sim 7\pi/12$ are in fact the boundaries of the 'intermediate regime' in which (Almog & Frankel 1995) the deterministic motion is characterized by the division of orientation space into separate domains of attraction corresponding to a number of simultaneously coexisting stable attractors. As a typical example, part (c) of Fig. 5 illustrates the variation of ϕ_c with λ for $\bar{\phi} = 5\pi/9$. A narrow intermediate interval of λ occurs in which ϕ_c is multiple-valued corresponding

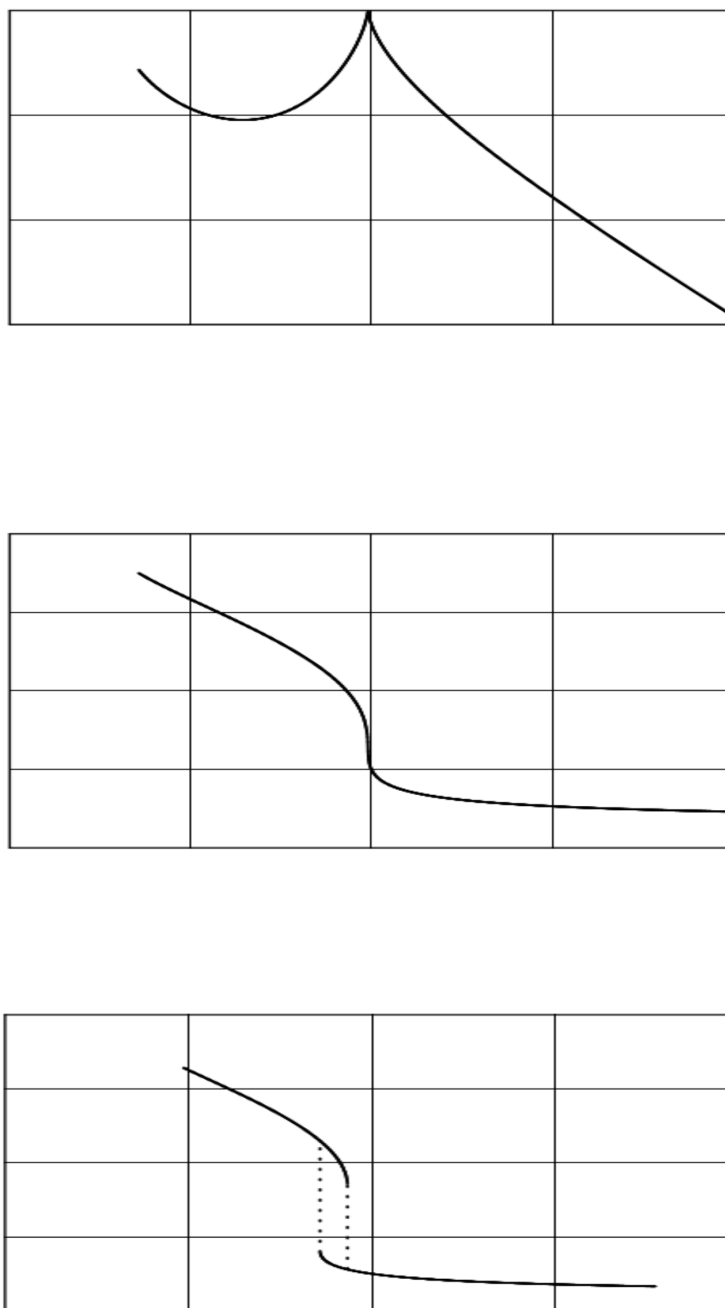


FIGURE 5. Illustration of deterministic motion of a prolate spheroid ($R = 3$) in the intermediate regime (Almog & Frankel 1995): (a) Variation with λ of the eigenvalue $(\partial\phi/\partial\phi)_c$ for $\bar{\phi} = 7\pi/12$; (b) Variation of ϕ_c with λ , $\bar{\phi} = 7\pi/12$; (c) Variation of ϕ_c for $\bar{\phi} = 5\pi/9$;

to the simultaneous coexistence of a pair of different stable equilibrium orientations.

It is interesting to note that, in the absence of diffusion, the variation of the bulk stress with λ exhibits the phenomenon of hysteresis, i.e. the bulk stress in the intermediate domain may depend on whether λ is being increased or decreased. The introduction of (however weak) rotary diffusion will render unique the orientational distribution which, in turn, may be obtained through an appropriate modification of the boundary-layer solution (3.19b) (cf. the conclusion of § 3.1.1.). Furthermore, the discontinuous change in ϕ_c across this intermediate interval is expected to be accompanied by rapid variations of $[\eta]$ with λ . It is remarkable that unlike the previously discussed cases (e.g. $\bar{\phi} = 0, 2\pi/3$) in which the limit when $\chi \rightarrow \infty$ of the bulk stress is regular and may directly be obtained from the deterministic problem [i.e. the leading-order terms in (4.36a)-(4.36d)], the present example shows that this limit is singular within the intermediate regime.

Figure 6 describes the effect of Pe on the variation of $[\eta]$ with λ for a prolate spheroid ($R = 3$) under the action of an external field whose azimuthal direction is $\bar{\phi} = 2\pi/3$ (cf. Fig. 3(f)). The solid lines correspond to the indicated values of Pe. The horizontal asymptotes respectively correspond to the limits Pe $\rightarrow 0$ for a finite λ ($\chi \rightarrow 0$, dash-dotted line), and $\lambda \rightarrow \infty$ (so that $\chi \rightarrow \infty$, dotted line). The asymptote (4.2a) for Pe $\rightarrow \infty$ has been omitted as it nearly coalesced with the curve representing Pe = 300.

The left and right horizontal asymptotes respectively correspond to a uniform orientational distribution, and a narrow boundary layer at $\phi_c = \bar{\phi} = 2\pi/3$. Since for the latter case dissipation rate is smaller than for a uniform distribution, the corresponding value of $[\eta]$ is smaller. At small Peclet numbers (Pe $\ll 1$) the suspension-orientational distribution monotonically evolves with increasing λ from a uniform distribution to a boundary layer about $\bar{\phi}$, hence the nearly monotonical variation of $[\eta]$ at Pe=1.

The variation of $[\eta]$ with Pe depends upon the value of λ . At relatively small values ($\lambda < \sim 0.1$) $[\eta]$ decreases with Pe since, as a result of the shear flow the prolate suspended particles tend to align with fluid velocity (Hinch & Leal 1972a). At intermediate values $\lambda \cong 1$ $[\eta]$ increases with Pe. This behaviour results from the appearance of boundary layers near $\phi_c \cong \pi$ (cf. the description of the curve $\bar{\phi} = 2\pi/3$ in Fig.4). Since for a given λ χ is proportional to Pe, these boundary layers become narrower with increasing Pe, i.e. more particles assume

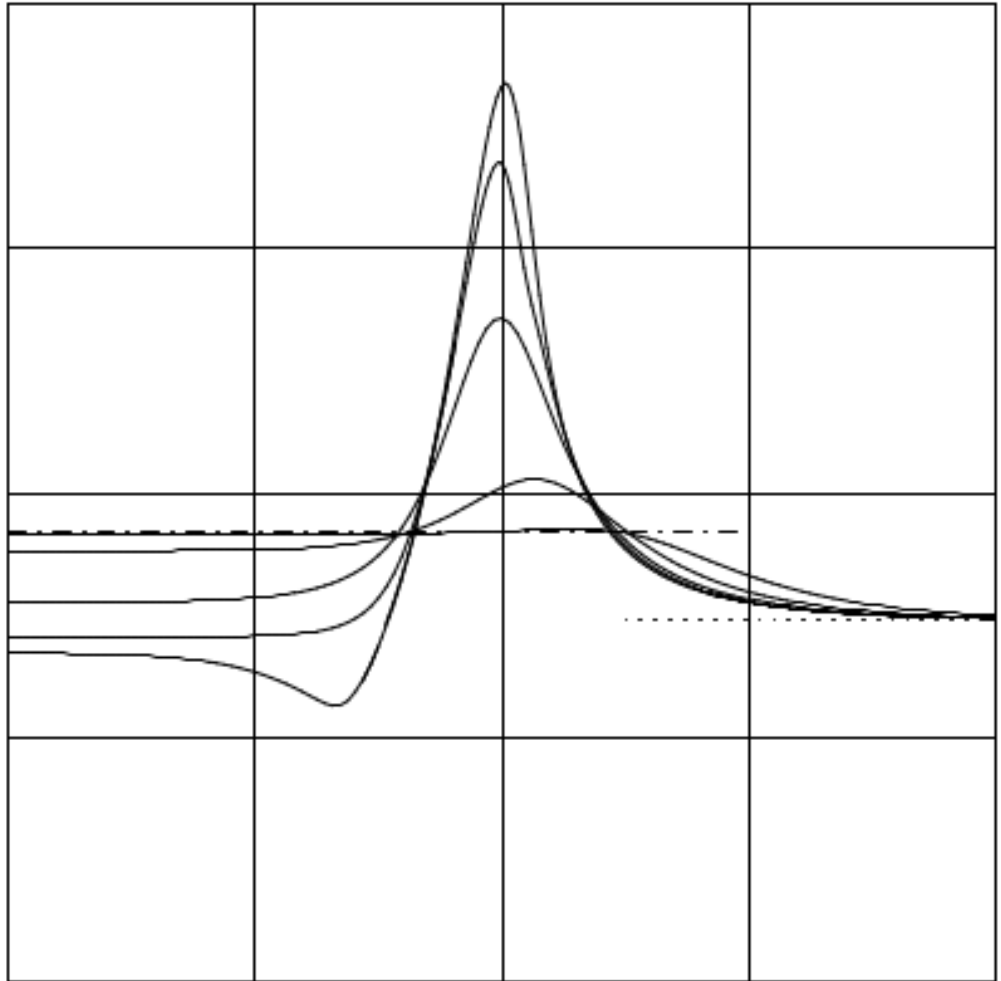


FIGURE 6. Variation with λ of $[\eta]$ at the indicated values of Pe for a suspension of prolate spheroids ($R = 3$) under external field acting in the plane for shear $\theta = \pi/2$ in the azimuthal direction $\bar{\phi} = 2\pi/3$. — exact (numerical) or boundary-layer approximation (4.36a); - - · - - - - $Pe \rightarrow 0$ and λ finite ($\chi \rightarrow 0$); ······ $\lambda, \chi \rightarrow \infty$.

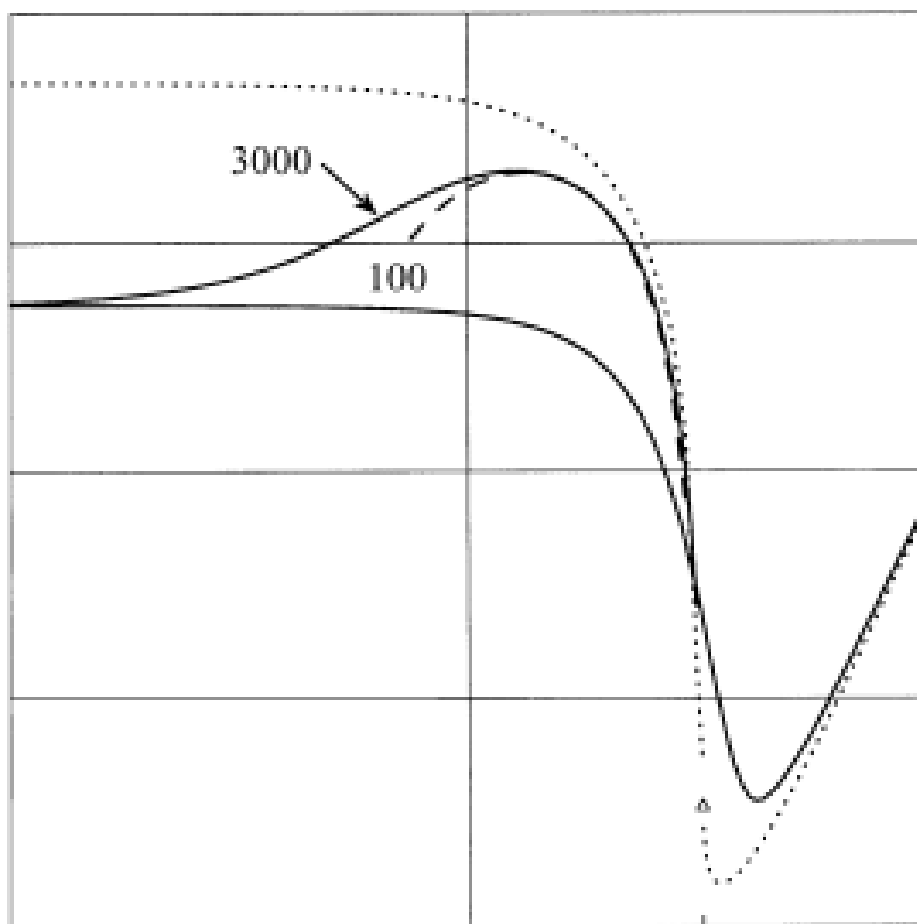


FIGURE 7. Variation of $[\eta]$ with λ for a suspension of prolate spheroids $R = \sqrt{3}$ for $\bar{\theta} = \pi/2$, and $\bar{\phi} = \pi/4$. — exact (numerical) solution for the indicated values of Pe , Δ saddle-node point, \cdots $Pe \rightarrow \infty$ asymptotes, - - - - - limit-cycle approximation for $Pe = 3000$.

the orientation perpendicular to the streamlines thereby increasing dissipation rate. For still larger values of λ , $\phi_c \rightarrow \bar{\phi} = 2\pi/3$, and $[\eta]$ accordingly converges to the right limit independently of Pe .

Discussion of the bulk stress has so far concentrated on cases of boundary-layer distributions about stable equilibrium orientations. We now briefly consider the case when a stable limit cycle exists. Calculation of the goniometric factors is accomplished by making use of (3.21) and (3.6) together with the first-order $O(Pe^{-1})$ correction (which has not explicitly been presented). Results are illustrated in Fig. 7 which

depicts the variation of $[\eta]$ with λ for a prolate spheroid $R = \sqrt{3}$ ($B=0.5$) and azimuthal direction of the external field $\bar{\phi} = \pi/4$. The solid lines represent the exact (numerical) solution for $Pe = 100, 3000$. The dotted curve and the triangle represent the leading-order $Pe \rightarrow \infty$ asymptotes. The triangle marks the value of $[\eta]$ at the saddle-node point appearing at $\lambda_b = 0.323$ [which value of $[\eta]$ is obtained from (3.28) and (3.30)]. The portion of the dotted line to the right of $\lambda = \lambda_b$ is the leading-order approximation (4.36a) for a boundary-layer about a stable node, whereas the left portion of this curve depicts the corresponding limit-cycle approximation (3.21) and (3.6). (The left portion of the dotted line terminates short of $\lambda = \lambda_b$ since the latter approximation becomes singular there.) The dashed curve is obtained from the limit-cycle approximation including the first-order $O(Pe^{-1})$ correction term for $Pe = 3000$. It is remarkable that even at such a large value of Pe , the correction term is still significant and is indeed necessary in order to achieve quantitative agreement with the exact solution. This agreement is limited to the rather narrow interval $\sim 0.12 < \lambda < \sim 0.30$. For smaller values of λ the limit cycle is insufficiently attractive to give rise to a narrow boundary-layer distribution. For larger values λ approaches the bifurcation at $\lambda = \lambda_b$ and the approximation becomes singular (cf. the conclusion of § 3.1.2).

Finally, it is interesting to note that Fig. 7 illustrates the singular behaviour in the limit when $\lambda \rightarrow 0$ and $Pe \rightarrow \infty$. Thus, toward the left margin of the figure, the dotted curve represents the limit $\lim_{\lambda \rightarrow 0} \{ \lim_{Pe \rightarrow \infty} [\eta] \} \cong 2.74$ whereas all solid curves eventually converge to $\lim_{Pe \rightarrow \infty} \{ \lim_{\lambda \rightarrow 0} [\eta] \} \cong 2.55$. The source of this difference is that when $\lambda \rightarrow 0$ for a finite fixed Pe then $\chi \rightarrow 0$ too. The corresponding deterministic rotary motion is periodic along Jeffery orbits and the limit $Pe \rightarrow \infty$ of the orientational distribution is given by the leading-order term in the expansion of Hinch & Leal (1972a). However, when $Pe \rightarrow \infty$ for a fixed (however small) value of λ , $\chi \rightarrow \infty$ as well and the deterministic motion is rather characterized by a limit cycle on $\theta = \pi/2$. The difference between both of the foregoing limit processes is also evident in Fig. 2. Thus, when $\lambda \rightarrow 0$ while $Pe (\gg 1)$ is fixed one is necessarily located in the dominant-shear domain. On the other hand, if $Pe \rightarrow \infty$ first we move to the right along a line of constant λ . Eventually, for Pe sufficiently large, we enter the domain ($\chi^2/Pe = \lambda^2 Pe \gg 1$) of dominant external field. No such a singular behaviour in the limit $\lambda \rightarrow 0$ exists in the case of dipolar spheres. When the external field acts in the plane of shear and $\lambda \rightarrow 0$ the deterministic rotary motion is periodic. Hence, no boundary-layer distribution can appear

and the bulk stress changes smoothly in the limit $\lambda \rightarrow 0$ independently of Pe .

The above discussion has concentrated on the variation of the intrinsic viscosity $[\eta]$. However, we emphasize that, once the orientational distribution has been obtained, the rest of the components of the bulk stress may similarly be studied. In this context, it seems worthwhile to mention that when $\chi, \lambda \rightarrow \infty$, $[\tau^a]$ converges to the nonzero limit (4.36d). This result is in contrast to the common opinion (e.g. Brenner 1970b, Leal 1971) that $[\tau^a]$ vanishes (presumably because $\langle \mathbf{e} \rangle \rightarrow \hat{\mathbf{F}}$) in this limit. While indeed $\left| \langle \mathbf{e} \rangle \times \hat{\mathbf{F}} \right| \sim O(\phi_c - \bar{\phi}) \sim O(\lambda^{-1})$ when $\chi, \lambda \rightarrow \infty$, [cf. the paragraph following (3.18a,b)], (4.1d) is proportional to $\lambda \langle \mathbf{e} \rangle \times \hat{\mathbf{F}}$, hence the external torque remains finite. In fact, as (4.36d) shows, the latter is equal to the hydrodynamic torque created by the shear flow. Obviously, in the absence of inertial effects both torques must balance each other.

As mentioned in the introduction, the numerical computation of Strand & Kim (1992) has so far been the only study of suspensions of dipolar axisymmetric particles which has not a priori been restricted to weak shear. We here focus on their figures 4 and 5 which (in the present notation) describe the variation with Pe of $[\eta] + [\tau^a]$ for a number of values of χ for a simple shear flow of a suspension of dipolar Brownian oblate spheroids ($R=0.4$) subject to an external field acting in the plane of shear in the respective azimuthal directions $\bar{\phi} = \pi/4$ and $\bar{\phi} = \pi/2$. Strand & Kim (1992) pointed out the maxima in the curves (of $[\eta] + [\tau^a]$) pertaining to $\chi > 2$ and attempted to provide an intuitive explanation for their occurrence by considering the behaviour of the particles in the limits $Pe \rightarrow 0, \infty$ ($\lambda \rightarrow \infty, 0$ respectively, for a fixed value of χ).

A correct qualitative explanation as well as an accurate quantitative prediction may, however, be obtained by means of the present analysis. Thus, by making use of (4.36a,4.36d), one readily finds that the above maxima occur at the respective Peclét numbers for which the equilibrium orientation is parallel to the streamlines, i.e., $\phi_c = 0$. (which for oblate spheroids corresponds to maximal hydrodynamic torque and dissipation rate). Furthermore, since for prescribed particle shape (R) and external field direction $\bar{\mathbf{e}}$, \mathbf{e}_c is exclusively determined by $\lambda = \chi/Pe$, Pe needs to vary with (sufficiently large) χ so as to maintain the constant value of λ for which $\phi_c = 0$. Indeed, the maxima in these figures correspond to nearly constant values of λ despite the rather moderate values of both Pe and χ . This accords with our numerical tests which verify that for $\chi = 10$, $\lambda = 1$ the deviation from the exact solution of

(4.36a)-(4.36d) including the first-order correction terms is less than 1 per cent. Use of (4.36a)-(4.36d) will in general become more advantageous with increasing χ or λ because its accuracy improves while the numerical scheme deteriorates. Finally, we note that the case $\bar{\phi} = \pi/2$ of Strand & Kim (1992) corresponds to $\bar{\phi} = \pi/2$ in the present study. (In the former case $\bar{\phi} = \pi/2$ corresponds to an external field acting perpendicularly to the streamlines of the ambient flow, however this is compensated by the fact that Strand & Kim (1992) consider oblate particles.) Thus the steep gradients occurring in their Fig. 5 are of similar origin as those appearing in our Fig. 3(d) and are related to the rapid variation of ϕ_c with λ in the intermediate regime discussed above.

5. CONCLUDING REMARKS

The present results assume a particularly simple and useful form when a single sufficiently stable equilibrium orientation \mathbf{e}_c exists in the corresponding deterministic problem. The bulk stress may then be obtained explicitly in terms of \mathbf{e}_c [cf.(4.36a)-(4.36d)]. Furthermore, validity of the results thus obtained is not restricted to weak shear $Pe \ll 1$, nor in fact even to $Pe \ll \chi$ for $\chi \gg 1$. Rather, \mathbf{e}_c is sufficiently stable to insure that (4.36a)-(4.36d) is an appropriate approximation for some $\lambda \sim O(1)$ (typically $\lambda > \sim 0.5$, cf. Fig. 3).

Comparison of Fig. 3 and Fig. 4 demonstrates that the use of (4.36a)-(4.36d) allows for a unified description as well as qualitative explanation of apparently different modes of variation of the bulk stress with intensity and direction of the external field. Moreover, for $\lambda \sim O(1)$ sufficiently large, the asymptotic expansions (4.36a)-(4.36d) are already accurate even at relatively moderate values of Pe and χ . (For instance, (4.36a)-(4.36d) including the first-order correction terms involve a relative error of less than 1 per cent for $Pe, \chi \approx 10$). They can thus successfully replace the numerical scheme which rapidly deteriorates with the onset of the steep gradients typical of orientational boundary layers.

The present analysis of the orientational distribution identifies the limits on the validity of the above boundary-layer approximation and facilitates discussion of the transition between the various asymptotic limits in terms of the corresponding deterministic particle rotary motion. This discussion is particularly important because some of these limits have counterparts neither in the problem of dipolar spheres nor in the case of torque-free axisymmetric particles. Thus (4.36a)-(4.36d) cease to be valid because the stable attractor may become insufficiently

strong, or may change its type (e.g. a limit cycle rather than a node), or else may not be unique. (Only the first of these has its parallel in the problem of dipolar spheres.)

We thus describe in terms of the deterministic motion the transition through the saddle-node bifurcation of the orientational distribution from a boundary layer about a stable equilibrium orientation to the relatively smooth distribution about a stable limit cycle. In the course of this transition the width of the boundary layer increases from $O(\text{Pe}^{-1/2})$ to $O(\text{Pe}^{-1/3})$ in the \mathbf{i}_ϕ azimuthal direction. Furthermore, unlike the usual exponential decay of boundary-layer distributions, the density of the bifurcation distribution only diminishes algebraically ($O(|\phi - \phi_b|^{-2})$) in the azimuthal direction. Finally, the analysis demonstrates the difficulty in obtaining accurate approximations when $\lambda \approx \lambda_b$, since the first-order correction to the bulk stress is relatively large $O(\text{Pe}^{-1/3})$ as opposed to the standard $O(\text{Pe}^{-1})$ correction.

Also interesting is the transition between the various boundary-layer approximations and the dominant-shear case. Thus, by considering the net average rotary flux induced by the external field, we explain the overlapping when $\bar{\theta} \neq \pi/2$ of the respective domains of validity in the (χ, Pe) plane of the boundary-layer and dominant-shear approximations. No such overlapping exists for $\bar{\theta} = \pi/2$ which is the source of the singularity of the double limit $\lambda \rightarrow 0, \text{Pe} \rightarrow \infty$. Depending upon the order in which these limits are taken, different bulk stresses are obtained (c.f. Fig.7). The difference is associated with the corresponding orientational distribution being either of boundary-layer type or an even dominant-shear distribution. No comparable singular behaviour occurs in dipolar spheres because their rotary motion possesses no limit cycles and is always periodic for $\lambda < 1/2$.

Particularly interesting phenomena are associated with the 'intermediate regime' where, for certain intervals of external-field directions and intensities, the phase space of the deterministic problem is divided into separate domains of attraction corresponding to a number of simultaneously coexisting stable attractors. Thus in this regime the variation with λ of the bulk stress will, in the absence of rotary diffusion, be discontinuous and exhibit hysteresis. Consequently, the limit of the macroscopic stress when $\chi \rightarrow \infty$ [for fixed $\lambda \sim O(1)$] is singular. These features explain the failure of (4.36a)-(4.36d) [e.g. for $\bar{\phi} = 7\pi/12$ in Fig. 4 and Fig. 3(e)] at the relatively large values of $\lambda \approx 1$ (when equilibrium orientations are presumably sufficiently attractive) as well as the observed drastic variations of the bulk stress with $\bar{\phi}$ and λ .

REFERENCES

- ALMOG, Y. & FRANKEL, I. 1995 The motion of axisymmetric dipolar particles in homogeneous shear flow. *J. Fluid Mech.* **289**, 243-261.
- BATCHELOR G. K. 1956 On steady laminar flow with closed streamlines at large Reynolds numbers. *J. Fluid Mech.* **1**, 177-190.
- BATCHELOR G. K. 1970 The stress system in a suspension of force-free particles. *J. Fluid Mech.* **41**, 545-570.
- BRENNER, H. 1970a Rheology of two-phase systems. *Ann. Rev. Fluid Mech.* **2**, 137-176.
- BRENNER, H. 1970b Rheology of a dilute suspension of dipolar spherical particles in an external field. *J. Colloid Interface Sci.* **32**, 141-158.
- BRENNER, H. 1972 Suspension rheology in the presence of rotary Brownian motion and external couples: elongational flow of dilute suspension. *Chem. Engng. Sci.* **27**, 1069-1107.
- BRENNER, H. 1974 Rheology of a dilute suspension of axisymmetric Brownian particles. *Int. J. Multiphase Flow*, **1**, 195-341.
- BRENNER, H. & CONDIFF, D.W. 1972 Transport mechanics is a system of orientable particles. III. Arbitrary particles. *J. Colloid Interface Sci.* **41**, 228-274.
- BRENNER, H. & CONDIFF, D.W. 1974 Transport mechanics is a system of orientable particles. IV. Convective transport. *J. Colloid Interface Sci.* **47**, 199-264.
- BRENNER, H. & WEISSMAN, M. H. 1972 Rheology of a dilute suspension of dipolar spherical particles in an external field. II. Effect of rotary Brownian motion. *J. Colloid Interface Sci.* **41**, 499-531.
- HALL, W. F. & BUSENBERG, S. N. 1969 Viscosity of magnetic suspensions. *J. Chem. Phys.* **51**, 137-144.
- HINCH, E. J. & LEAL, L. G. 1972a The effect of Brownian motion on the rheological properties of a suspension of non-spherical particles. *J. Fluid Mech.* **52**, 683-712.
- HINCH, E. J. & LEAL, L. G. 1972b Note on the rheology of a dilute suspension of dipolar spheres with weak Brownian couples. *J. Fluid Mech.* **56**, 803-813.
- JANSONS, K. M. 1983 Determination of the constitutive equations for a magnetic fluid. *J. Fluid Mech.* **137**, 187-216.
- JEFFERY, G. B. 1922 The motion of ellipsoidal particles immersed in a viscous fluid. *Proc. Roy. Soc. Lond.* **A102**, 161-179.
- JHON, M. S., KWON, T. M., CHOI, H. J., & KARIS, T. E. 1996 Microrheological study of magnetic particle suspensions. *Ind. Eng. Chem. Res.* **35**, 3027-3031.
- LEAL, L. G. 1971 On the effect of particle couples on the motion of a dilute suspension of spheroids. *J. Fluid Mech.* **46**, 395-416.
- LEAL, L. G. & HINCH, E. J. 1971 The effect of weak Brownian rotations on particles in shear flow. *J. Fluid Mech.* **46**, 685-703.
- PEDLEY, T. J. & KESSLER, J. O. 1990 A new continuum model for suspensions of gyrotactic micro-organisms. *J. Fluid Mech.* **212**, 155-182.
- PEDLEY, T. J. & KESSLER, J. O. 1992 Hydrodynamic phenomena in suspensions of swimming micro-organisms. *Ann. Rev. Fluid Mech.* **24**, 313-358.
- ROSENSWEIG, R. E. 1985 *Ferrohydrodynamics*. Cambridge University Press.
- SALUEÑA, C. PÉREZ-MADRID, A. & RUB'I, J. M. 1994 The viscosity of a suspension of rod-like particles. *J. Colloid Interface Sci.* **164**, 269-279.

SHLIOMIS, M. I. 1972 Effective viscosity of magnetic suspensions. *Soviet Physics JETP*, **34**, 1291-1294.

SMITH, T.L. & BRUCE, C.A. 1979 Intrinsic viscosities and other rheological properties of flocculated suspensions of nonmagnetic and magnetic ferric oxides. *J. Colloid Interface Sci.* **72**, 13-26.

STRAND, S.R. & KIM, S. 1992 Dynamics and rheology of a dilute suspension of dipolar nonspherical particles in an external field: Part 1. Steady shear flows. *Rheol. Acta*, **31**, 94-117.

¹DEPARTMENT OF APPLIED MATHEMATICS AND COMPUTER SCIENCE, THE WEIZMANN INSTITUTE OF SCIENCE REHOVOT 76100, ISRAEL, ²FACULTY OF AEROSPACE ENGINEERING, TECHNION - ISRAEL INSTITUTE OF TECHNOLOGY HAIFA 32000, ISRAEL